# Specific TRPC6 Channel Activation, a Novel Approach to Stimulate Keratinocyte Differentiation\*S

Received for publication, March 6, 2008, and in revised form, September 24, 2008 Published, JBC Papers in Press, September 25, 2008, DOI 10.1074/jbc.M801844200

Margarethe Müller<sup>‡</sup>, Kirill Essin<sup>§</sup>, Kerstin Hill<sup>¶</sup>, Heike Beschmann<sup>||</sup>, Simone Rubant<sup>||</sup>, Christoph M. Schempp\*\*, Maik Gollasch<sup>§</sup>, W. Henning Boehncke<sup>||</sup>, Christian Harteneck<sup>¶</sup>, Walter E. Müller<sup>‡</sup>, and Kristina Leuner<sup>‡1</sup>

From the <sup>‡</sup>Institute of Pharmacology, Biocenter Niederursel, Johann Wolfgang Goethe-University, Max-von-Laue-Strasse 9, 60439 Frankfurt, Germany, the <sup>§</sup>Charité University Medicine, Section Nephrology/Intensive Care, Campus Virchow, and Franz Volhard Clinic at the Max Delbrück Center Berlin-Buch, Augustenburger Platz 1, 13353 Berlin, Germany, and the <sup>¶</sup>Molecular Pharmacology and Cell Biology, Charité, 14195 Berlin, Germany; <sup>||</sup>Department of Dermatology, Johann Wolfgang Goethe-University; Theodor-Stern-Kai 7, 60590 Frankfurt, Germany, and the \*\*Department of Dermatology, University Medical Center Freiburg, 79104 Freiburg, Germany

The protective epithelial barrier in our skin undergoes constant regulation, whereby the balance between differentiation and proliferation of keratinocytes plays a major role. Impaired keratinocyte differentiation and proliferation are key elements in the pathophysiology of several important dermatological diseases, including atopic dermatitis and psoriasis. Ca2+ influx plays an essential role in this process presumably mediated by different transient receptor potential (TRP) channels. However, investigating their individual role was hampered by the lack of specific stimulators or inhibitors. Because we have recently identified hyperforin as a specific TRPC6 activator, we investigated the contribution of TRPC6 to keratinocyte differentiation and proliferation. Like the endogenous differentiation stimulus high extracellular Ca2+ concentration ([Ca2+]o), hyperforin triggers differentiation in HaCaT cells and in primary cultures of human keratinocytes by inducing Ca2+ influx via TRPC6 channels and additional inhibition of proliferation. Knocking down TRPC6 channels prevents the induction of Ca2+- and hyperforin-induced differentiation. Importantly, TRPC6 activation is sufficient to induce keratinocyte differentiation similar to the physiological stimulus [Ca<sup>2+</sup>]<sub>a</sub>. Therefore, TRPC6 activation by hyperforin may represent a new innovative therapeutic strategy in skin disorders characterized by altered keratinocyte differentiation.

Our skin undergoes constant regulation to provide a protective epithelial barrier, whereby the differentiation of keratinocytes from proliferating cells in the basal layer into platted, dead cells in the stratum corneum plays a major role. Keratinocytes leaving the basal layer not only change structure and shape but also loose their ability to proliferate and enter the terminal dif-

ferentiation stage by expressing proteins required for the cornification like keratin 1 (K1)<sup>2</sup> or keratin 10 (K10) and additional structural proteins that are needed for the cornification such as involucrin (IVL) or transglutaminase (1). The precise balance between proliferation and differentiation found in healthy individuals is altered in individuals suffering from various skin diseases like psoriasis or atopic dermatitis (AD). Psoriasis is marked by thickened epidermis because of increased proliferation but disturbed differentiation of keratinocytes (2). Accordingly, psoriatic skin is characterized by reduced differentiation markers but elevated epidermal proliferation markers (3). Psoriatic plaques are covered by a thick layer of scales caused by aberrant terminal differentiation. The granular layer of the epidermis, in which the terminal differentiation begins, is greatly reduced or absent in psoriatic lesions, which results in a stratum corneum consisting of incompletely differentiated keratinocytes.

As for psoriasis, the exact pathomechanisms of AD are not known (4). In addition to an enhanced immune response, a reduced integrity of the epidermal barrier seems to be relevant. Proksch *et al.* (5) suggested that a disturbed differentiation of keratinocytes causes a defective skin barrier function in AD, enabling the enhanced penetration of environmental allergens. An impaired expression of cornified envelope proteins like involucrin and keratins like K10, important for permeability barrier formation, could also be detected in lesional skin from patients with AD (6). However, other factors not directly related to keratinocyte function seem to contribute to the altered skin barrier seen in AD patients, *e.g.* a mutation in the structural protein filaggrin (7).

Because of the crucial role of keratinocyte differentiation for normal skin function and as relevant pathomechanism in various skin diseases, an exact knowledge of the mechanism relevant for the specific and tight sequence of events leading to keratinocytes proliferation and differentiation is very much

<sup>&</sup>lt;sup>2</sup> The abbreviations used are: K1, keratin 1; K10, keratin 10; IVL, involucrin; AD, atopic dermatitis; TRPC, canonical transient receptor potential; TRPV, vanilloid-like transient potential channel; hPK, human primary keratinocytes; YFP, yellow fluorescent protein; DN, dominant negative; RT, reverse transcription; siRNA, small interfering RNA; GAPDH, glyceraldehyde-3-phosphate dehydrogenase; MTT, 3-[4,5-dimethylthiazol-2-yl]-2,5-diphenyltetrazolium bromide; RNAi, RNA interference; MES, 4-morpholineethanesulfonic acid.



<sup>\*</sup> This work was supported by a research grant from Casella Med GmbH & Co. KG (Cologne, Germany) and the German Research Foundation. The costs of publication of this article were defrayed in part by the payment of page charges. This article must therefore be hereby marked "advertisement" in accordance with 18 U.S.C. Section 1734 solely to indicate this fact.

The on-line version of this article (available at http://www.jbc.org) contains supplemental Fig. S1.

<sup>&</sup>lt;sup>1</sup> To whom correspondence should be addressed: Institute of Pharmacology, Biocenter Niederursel, Johann Wolfgang Goethe-University, Max-von-Laue-Str. 9, 60439 Frankfurt, Germany. Tel.: 49-69-79829365; Fax: 49-69-79829374; E-mail: Leuner@em.uni-frankfurt.de.

needed. On a cellular level, several studies clearly showed that Ca<sup>2+</sup> plays a crucial role in the regulation of keratinocyte differentiation especially for the terminal stages like cell stratification and cornification (8). Induction of differentiation and inhibition of proliferation are tightly regulated by an increase in [Ca<sup>2+</sup>], because of both Ca<sup>2+</sup> release and Ca<sup>2+</sup> influx mechanisms with a still unknown molecular basis. In tissue culture, the differentiation of keratinocytes can be triggered by experimentally increasing  $[Ca^{2+}]_o$  above 0.1 mm (9). In a first step, this elevation in [Ca<sup>2+</sup>]<sub>a</sub> induces a rise in [Ca<sup>2+</sup>]<sub>i</sub> by activating the Ca<sup>2+</sup>-sensing receptor, a G-protein-coupled receptor (10). In the next step, stimulation of the Ca<sup>2+</sup>-sensing receptor activates the phospholipase C pathway generating inositol 1,4,5triphosphate and diacylglycerol (8). Both intracellular second messengers elevate intracellular Ca<sup>2+</sup> concentration. Inositol 1,4,5-triphosphate as a ligand of inositol 1,4,5-triphosphate receptors induces the release of Ca<sup>2+</sup> from the endoplasmic reticulum. Diacylglycerol directly activates members of the canonical transient receptor potential (TRPC) channel family. Based on the sequence homology, activation mechanism, and ability to form heteromeric channel complexes, the proteins of the TRPC group can be divided into the TRPC1, TRPC4, and TRPC5 and the TRPC3, TRPC6, and TRPC7, of which diacylglycerol directly activates only TRPC3, TRPC6, and TRPC7 (11). However, the data about the specific TRPC channels relevant for keratinocyte differentiation are controversial. For example Cai et al. (12) detected TRPC1, TRPC5, TRPC6, and TRPC7 in gingival keratinocytes, whereas Beck et al. (13) showed the expression of TRPC1, TRPC4, TRPC5, and TRPC7 in HaCaT keratinocytes. Similarly, TRPC1 as well as TRCP4 have been implicated in the Ca<sup>2+</sup>-sensing receptor triggered elevation of [Ca<sup>2+</sup>], (14, 15). Moreover, following Ca<sup>2+</sup>-stimulated differentiation of gingival keratinocytes, elevated expression of TRPC1, TRPC5, TRPC6, and TRPC7 has been reported (12).

The attempts to identify the Ca<sup>2+</sup> channels playing the major role for Ca<sup>2+</sup>-sensing receptor-mediated keratinocyte differentiation have been significantly hampered by the lack of pharmacological tools specifically affecting individual TRPC channel function. However, because we have recently identified hyperforin as a specific and potent TRPC6 activator (16, 17), we were able for the first time to investigate in detail the specific contribution of this channel for Ca2+-mediated keratinocyte differentiation. Our findings not only show that TRPC6 plays a role but also demonstrate that the specific activation of TRPC6 alone is sufficient for nearly full physiological response. TRPC6 activation by hyperforin or similar compounds therefore represents a novel approach to pharmacologically activated keratinocyte differentiation.

To elucidate the molecular mechanism for keratinocyte differentiation in culture, we used HaCaT cells as established and characterized cell model and human primary keratinocytes (hPKs) and human skin explants as native systems to validate our data. By this approach, we were able to show that both cell types express functionally active TRPC6 channels in vitro and ex vivo. Furthermore, the use of hyperforin, the recently identified selective activator of TRPC6, enabled us to show that the Ca<sup>2+</sup>-induced differentiation of keratinocytes is to a large extent mediated by TRPC6 channels. The elucidation of this molecular pathway has several clinical implications. First, the TRPC6 gene is an interesting candidate gene for genetic approaches, and second stimulating TRPC6 channels may be a novel treatment approach in dermatology.

#### **EXPERIMENTAL PROCEDURES**

Sources and Preparation of Reagents—Hyperforin was a kind gift from Dr. Willmar Schwabe (Karlsruhe, Germany). Fluorescence dyes (SBFI-AM and fura-2-AM) were purchased from Molecular Probes (Eugene, OR). Pluronic F-127, 2-aminophenoxyborate (Tocris, Abvonmouth, UK), and SK&F 96365 (Biotrend, Cologne, Germany) were used from 10 mm stock solution in dimethyl sulfoxide. N-(p-Amylcinnamoyl) anthranilic acid (Calbiochem, San Diego, CA) was used from 50 mm stock solution in dimethyl sulfoxide. GdCl<sub>2</sub> and LaCl<sub>2</sub> (Sigma-Aldrich) were dissolved in H<sub>2</sub>O prior to experiments.

Cell Culture—The HaCaT human keratinocyte cell line was cultured in keratinocyte-SFM medium (Invitrogen) with 10% heat-inactivated fetal calf serum (Sigma-Aldrich), 50 units/ml penicillin (Sigma-Aldrich), and 50 μg/ml streptomycin (Sigma-Aldrich). Human primary keratinocytes were derived from adult skin and cultured according to the method of Rheinwald and Green (18) in keratinocyte growth medium (Promo Cell, Heidelberg, Germany). HaCaT cells and hPKs were cultured under a 5% CO<sub>2</sub> humidified atmosphere at 37 °C. For the experiments, the cells were seeded in 6-well plates for RT-PCR and Western blot and on glass coverslips for histochemistry and Ca<sup>2+</sup> imaging. For differentiation studies, the cells were allowed to attach for 24 h after trypsinization, and then 0.1 mm Ca<sup>2+</sup>-containing keratinocyte-SFM medium was replaced by SFM medium with 2 mm  $Ca^{2+}$  or hyperforin 1  $\mu$ m. After 48 – 72 h of incubation in the latter medium, histochemical staining, RT-PCR, and Western blotting of corresponding markers were performed.

Split Thickness Skin Organ Culture—6-mm punch biopsies containing epidermis and papillary dermis were obtained from dermatome-separated human skin. The biopsies were floated on SFM in six-well plates in the presence of Ca<sup>2+</sup>-free medium (negative control),  $\bar{2}$  mM Ca<sup>2+</sup> (positive control), or 1  $\mu$ M hyperforin. After 24 h the cultures were terminated, fixed in paraformaldehyde, and embedded in paraffin. 3-µm sections were stained for TRPC6 using the labeled streptavidin biotin method as described (19). Five random fields of sections from four independent skin explants were counted for TRPC6-positive keratinocytes at ×400 magnification. The final count/ group represents the mean  $\pm$  S.D.

Cell Transfection-HaCaT keratinocytes and hPKs were plated in 6-well plates onto glass coverslips and transiently transfected 24 h later by the addition of a transfection mixture containing 0.5 µg of DNA and 1 µl of FuGENE 6 transfection reagent (Roche Applied Science) in 97 µl of Opti-MEM medium (Invitrogen). The cDNA constructs have been kindly provided by Dr. Michel Schaefer (11). Ca<sup>2+</sup> imaging was conducted 2 days after transfection. Histochemical staining, RT-PCR, and Western blotting were conducted 2-3 days after transfection. For TRPC knockdown studies with siRNA, HaCaT cells were plated in 6-well plates onto glass coverslips and transiently transfected 24 h later by the addition of trans-



**TABLE 1**Primer and siRNA sequences

No.	Name	Accession no.	Forward $(5' \rightarrow 3')$	Backward $(5' \rightarrow 3')$	Expected size
					bp
1	K1	NM_006112	GGACATGGTGGAGGATTACCG	TGCTCTTCTGGGCTATATCCTCG	316
2	K10	NM_000421	GCAAAATCAAGGAGCGGTATGA	GAGCTGCACACAGTAGCGACC	685
3	IVL	NM_005547	TCTAAGATGTCCCAGCAACACA	TCATGCTGTTCCCAGTGCTGTT	292
4	TGM I	NM_000359	GATCGCATCACCCTTGAGTTAC	TCCTCATGGTCCACGTACACAAT	304
5	TRPC1	Z73903	ATGTATACAACCAGCTCTATCTTG	AGTCTTTGGTGAGGGAATGATG	525
6	TRPC3	U47050	CTGCAAATGAGAGCTTTGGC	AACTTCCATTCTACATCACTGTC	388
7	TRPC4	AF175406	ATTCATATACTGCCTTGTGTTG	GGTCAGCAATCAGTTGGTAAG	329
8	TRPC5	AF054568	ACTTCTATTATGAAACCAGAGC	GCATGATCGGCAATAAGCTG	289
9	TRPC6	AF080394	AAGACATCTTCAAGTTCATGGTC	TCAGCGTCATCCTCAATTTCC	322
10	TRPC7	AJ272034	GTCCGAATGCAAGGAAATCT	TGGGTTGTATTTGGCACCTC	477
11	TRPC1 siRNA		5'-GAUCUGUCAAAAUUCCGAATT-3'	5'-UUCGGAAUUUUGACAGAUCTT-3'	
12	TRPC3 siRNA		5'-CGUUAUCAGCAGAUAAUGATT-3'	5'-UCAUUAUCUGCUGAUAACGTG-3'	
13	TRPC4 siRNA		5'-GUAUAGACUAUGAUCUAAATT-3'	5'-UUUAGAUCAUAGUCUAUACTA-3'	
14	TRPC5 siRNA		5'-CACCCUGAUUCAUCCGAGATT-3'	5'-UCUCGGAUGAAUCAGGGUGGT-3'	
15	TRPC6 siRNA 1		5'-UCUCUCCAUUUGGUAUGAGAAUCUU-3'	5'-AAGAUUCUCAUACCAAUGGAGAGA-3'	
16	TRPC6 siRNA 2		5'-CCCAAGGAAUAUUUGUUUGAGUUGA-3'	5'-ACAACUCAAACAAAUAUUCCUUGGG-3'	
17	TRPC6 siRNA 3		5'-GGAGCUCAGAAGAUUUCCAUCUAAA-3'	5'-UUUAGAUGGAAAUCUUCUGAGCUCC-3'	
18	TRPC7 siRNA		5'-CCAUAUUCGGCUUAUCUGAAGUAAU-3'	5'-AUUACUUCAGAUAAGCCCGAAUAUGG-3'	

fection mixture containing 100 nm TRPC6 siRNA (Invitrogen) or 25 nm TRPC1, TRPC3, TRPC4, TRPC5, and TRPC7 siRNA (Ambion) and 2.5  $\mu$ g/ml Lipofectamine 2000 (Invitrogen) in 250  $\mu$ l of Opti-MEM medium. As a control 100 nm siRNA control sequence with low GC content (Invitrogen) or 25 nm negative RNAi control (Ambion) with their complementary sequences were transfected in the same procedure. Histochemical staining and Western blotting were performed 2–3 days after transfection.

RT-PCR—RNA was isolated using TRIzol reagent (Invitrogen), chloroform, and 100% ethanol according to the manufacturer's instructions. The reactions were carried out using 2  $\mu$ g of mRNA. First strand cDNA was synthesized from 2  $\mu$ g of total RNA in a 20-µl final volume using a first strand cDNA synthesis kit (Invitrogen). After reverse transcription, amplification was carried out by PCR using Taq DNA polymerase and dNTP set of Invitrogen. A 2-µl aliquot of the reverse transcription solution was used as a template for specific PCR. The PCR primers used to amplify TRPC1, 3, 4, 5, 6, and 7 channels, IVL, TGM I, K1, and K10 cDNAs are specified in Table 1. Commercially available 18 S rRNA primers (Ambion, Huntington, UK) were used as internal loading control, and the predicted 18 S (Classic II) band size was 324 bp. The PCR was conducted under the following conditions: an initial denaturation step at a temperature of 94 °C for 5 min and 30 cycles as follows: 30 s at 94 °C, 30 s at 58 °C, 30 s at 72 °C, and finally 7 min at 72 °C. PCR products were run on a 1% agarose gel and stained with ethidium bromide. Changes in relative mRNA levels were obtained by relating each PCR product to its internal control. After gel electrophoresis, quantification was archived with Easywin 32 software (Herolab). RT-PCR analysis using TRPC6-specific primer resulted in a fragment of the expected size of 322 bp. The sequence of fragment was sequenced (Seqlab, Göttingen, Germany) and corresponded to the TRPC6 sequence available in GenBank<sup>TM</sup> under accession number AF080394.

Western Blotting—HaCaT cells and hPKs were harvested by centrifugation (800  $\times$  g, 5 min, room temperature). The cells were resuspended in lysis buffer (50 mM Tris/HCl, 2 mM dithiothreitol, 0.2  $\mu$ M benzamidine, 1 mM EDTA, pH 8.0) and homogenized by shearing through 26-gauge needles. After

removal of nuclei ( $800 \times g$ , 2 min, 4 C), the supernatants were mixed with gel loading buffer (62.5 mM Tris/HCl, 10% glycerol, 5% mercaptoethanol, 2% SDS, 0.02% bromphenol blue, pH 6.8). After electrophoresis, the proteins were transferred on nitrocellulose membrane. The membrane was incubated with a blocking solution (Invitrogen) for 2 h and overnight and then probed with using specific rabbit polyclonal anti-TRPC6 (Chemicon, 1/300), mouse monoclonal anti-cytokeratin 1/10 (Chemicon, 1/200), and mouse monoclonal anti-GAPDH (Chemicon, 1/300). The antibodies were visualized by incubation with horseradish antibody conjugate. To calculate the ratio between TRPC6, cytokeratin 1/10 and GAPDH band intensities we used Image J.

Histochemistry—HaCaT cells grown on glass coverslips were washed twice with phosphate-buffered saline, fixed in 4% paraformaldehyde in phosphate-buffered saline, and stained with Mayer's hematoxylin and eosin solutions. Morphological changes were analyzed by using Nikon NIS Elements AR 2.1 software.

For cytospin experiments, subconfluent hPKs were incubated with SFM containing Ca<sup>2+</sup>-free medium (negative control), 2 mm Ca<sup>2+</sup> (positive control), or 1  $\mu$ m hyperforin. After 24 h the cells were trypsinized, washed twice in phosphate-buffered saline, and centrifuged onto coated microscope slides using a cytospin centrifuge (Thermo Shandon, UK). The cells were fixed with 2% formaldehyde. Subsequently the cells were stained for TRPC6 using the labeled streptavidin biotin method according to the manufacturer's instruction (DCS, Hannover, Germany). The primary polyclonal TRPC6 antibody (Chemicon) and the secondary biotinylated multi-link antibody (Dako, Denmark) were used at a dilution of 1:200.

Fluorescence Measurements—The intracellular  $Ca^{2+}$  concentration  $[Ca^{2+}]_i$ , barium  $[Ba^{2+}]_i$ , strontium  $[Sr^{2+}]_i$ , and sodium  $[Na^+]_i$  measurements in single cells were carried out using the fluorescence indicators fura-2-AM or SBFI-AM in combination with a monochromator-based imaging system (T.I.L.L. Photonics, Martinsried, Germany or Attofluor Ratio Vision System) attached to an inverted microscope (Axiovert 100; Carl Zeiss, Oberkochen, Germany). For  $[Ca^{2+}]_i$  measurements HaCaT cells and hPKs were loaded with 4  $\mu$ M fura-2-AM



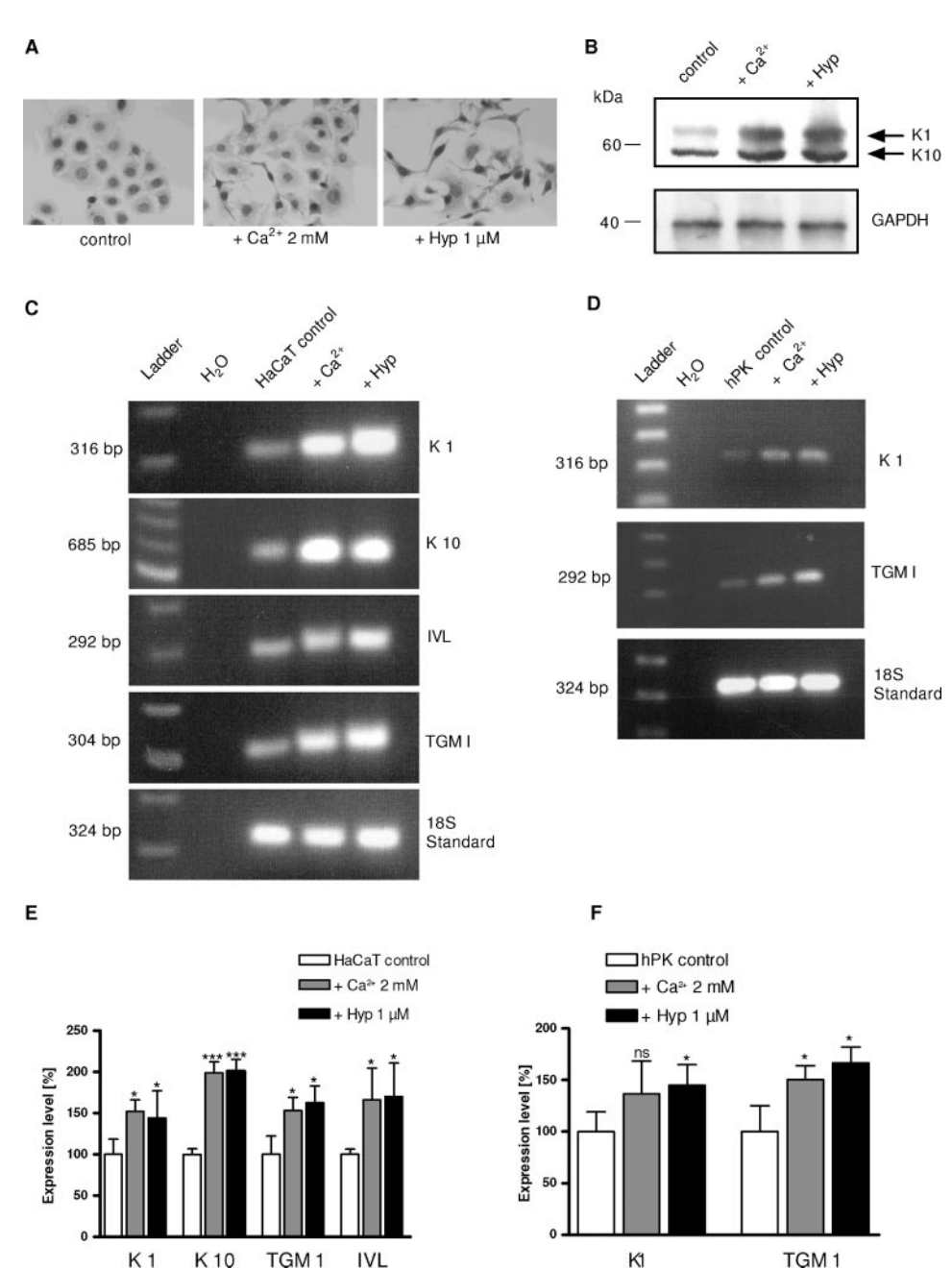


FIGURE 1. Hyperforin induces differentiation in HaCaT keratinocytes and hPKs. Both cell types were treated with  $Ca^{2+}$  (2 mm) and hyperforin (Hyp, 1  $\mu$ m) for 3 days. A, after the incubation period, cells were stained with Mayer's hematoxylin and eosin solutions. Representative images of HaCaT cells are shown from at least three experiments. B, Western blotting of differentiation marker proteins K1 and K10. Comparability was achieved by GAPDH-normalizing of protein load. Shown is a representative blot from a single experiment that was repeated three times. Total mRNA of treated HaCaT cells (C) or hPKs (D) was isolated, reverse transcribed, and subjected to PCR. The expression of differentiation markers in untreated and with hyperforin (1 µм) or Ca<sup>2+</sup> (2 mm) differentiated HaCaT keratinocytes was analyzed. E and F, histograms showing relative expressing levels of differentiation markers in HaCaT keratinocytes (E) and hPKs (F), compared with their normalized expression levels in untreated control cells. The asterisks denote statistical significance as compared with control HaCaT keratinocytes or hPKs (n = 3; \*, p < 0.1, unpaired t test).

(Invitrogen) and 0.01% Pluronic F-127 (Invitrogen) for 30 min at room temperature in a standard solution composed of 138 mм NaCl, 6 mм KCl, 1 mм MgCl<sub>2</sub>, 2 mм CaCl<sub>2</sub>, 5.5 mм glucose, and 10 mm HEPES (adjusted to pH 7.4 with NaOH). The coverslips were then washed in this buffer for 20 min and mounted in a perfusion chamber on the microscope stage. To measure Ba<sup>2+</sup> and Sr<sup>2+</sup> influx, the cells were incubated with Ca<sup>2+</sup>-free

standard solution. The influx of  $\mathrm{Ba}^{2+}$  and  $\mathrm{Sr}^{2+}$  in HaCaT cells was evaluated in fura-2-loaded cells by measuring the fluorescence of Ba<sup>2+</sup>/Sr<sup>2+</sup> fura complexes. [Na<sup>+</sup>], concentration was measured by incubating HaCaT cells with the fluorescence dye SBFI-AM (10 μM) and 0.01% Pluronic F-127 for 40 min at room temperature in a sodiumfree medium (3 mm KCl, 2 mm MgCl, 5 mm Tris, 10 mm glucose; the sodium replaced by an equimolar amount of sucrose; pH adjusted with HCl to 7.4). After washing out the fluorescence dye, sodium-containing medium (140 mm Na<sup>+</sup>) was added. For all of the fluorescence experiments, fluorescence excited at 340 and 380 nm. After correction for background fluorescence, the fluorescence ratio  $F_{340}/$  $F_{380}$  was calculated. In all of the experiments, transfected cells (5-10 cells) of the whole field of vision were identified by their YFP fluorescence at an excitation wavelength of 480 nm.

Electrophysiology-Currents in HaCaT cells were recorded in the perforated patch configuration with amphotericin B. The experiments were performed at room temperature using a Axopatch 200B amplifier (Axon Instruments). Patch pipettes of 3-5 MOhm were fabricated from borosilicate glass capillaries. The bath solution consisted of 6 mm KCl, 134 mm NaCl, 1 mm MgCl<sub>2</sub>, 2 mm CaCl<sub>2</sub> 10 mm HEPES, 10 mm D-Glucose, 40 mm D-mannitol (pH 7.4, NaOH). The pipette solution contained 134 mm Cs-MES, 6 mm KCl, 10 mm NaCl, 1 mm MgCl<sub>2</sub>, 0.1 mm EGTA, 10 mm HEPES (pH 7.2, CsOH). Amphotericin B (Sigma) were dissolved in dimethyl sulfoxide and diluted into the pipette solution to give a final concentration of 250 µg/ml. Perforation

started shortly after seal formation and reached a steadystate level within 5-10 min. The currents were recorded from holding potentials of -40 mV during linear voltage ramps at 0.67 V/s from -100 mV to +100 mV applied each 15 s. The average capacitance of the cells was 30.7  $\pm$  1.4 pF (n = 39). Patch pipettes of 3–5 M $\Omega$  were fabricated from borosilicate glass capillaries. The experiments were analyzed



using Clampfit software (Axon Instruments). The data are presented as the means  $\pm$  S.E.

Proliferation Measurement—Quantification of cell proliferation was determined by a nonisotopic immunoassay kit (Calbiochem, Germany), based on the measurement of bromode-oxyuridine incorporation during DNA synthesis. The assay was carried out according to the product instruction manual.

MTT Assay—Estimation of cytotoxicity of hyperforin on cell viability was determined by means of MTT assay, on HaCaT keratinocytes grown on 96-well plates, after 48 h of treatment. According to the manufacturing instructions (Roche Applied Science), MTT reagent was added at a final concentration of 1 mg/ml. Incubation was continued for another 2 h, and the formazan crystals were then solubilized by  $100 \, \mu l$  of a  $20\% \, SDS/50\% \, N,N$ -dimethyl-formamide solution. After complete  $12 \, h$  of solubilization, the absorption was measured at  $550 \, h$  m with a correction wavelength of  $620 \, h$  m using an enzyme-linked immunosorbent assay micro plate reader.

Statistics—In addition to Microsoft Office Excel, GraphPad PRISM<sup>TM</sup> (version 3.0) was used for statistical analyses and to create the graphs. For statistical analyses, an unpaired Student's t test (two-tailed) was used. The data are expressed as the means  $\pm$  S.D.

#### **RESULTS**

Hyperforin Induces Differentiation in HaCaT Keratinocytes— Because of the unclear situation of TRPC channels expressed in keratinocytes, we performed RT-PCR analyses from RNA extracted from primary keratinocytes and HaCaT cells. The detection of TRPC6-encoding mRNA in both cell types provided the rationale to use hyperforin as pharmacological tools to unravel the mechanism of keratinocyte differentiation induced by high (2 mm) extracellular calcium (high  $[Ca^{2+}]_a$ ), which has been shown to be an endogenous trigger (1, 20). In the initial experimental set up, we compared cell morphology as read out in hyperforin-treated cells and cells exposed to high  $[Ca^{2+}]_{a}$  (Fig. 1A). Control HaCaT keratinocytes and hPKs are predominantly polygon-shaped, with clear boundaries and a large nucleus/cytoplasm ratio (Fig. 1A, left panel). After a period of 3 days in the presence of high [Ca<sup>2+</sup>]<sub>o</sub>, the cells undergo visible morphological changes, from large and flat to closely associated, elongated cells with spider web morphology (Fig. 1A, middle panel). As shown in Fig. 1A (right panel) for HaCaT cells, hyperforin induced morphological changes in HaCaT and hPK cells (data not shown), which are comparable with the morphology of cells cultured in the presence of high  $[Ca^{2+}]_o$  (compare *middle* and *right panels*). To test whether or not these morphological changes can also be detected by biochemical methods, we analyzed protein extracts of hyperforinand high [Ca<sup>2+</sup>]<sub>a</sub>-treated cells (Fig. 1*B*). Western blot analyses revealed that HaCaT and hPK cells express basal levels of K1 and K10 being up-regulated during high [Ca<sup>2+</sup>]<sub>o</sub> or hyperforin treatment. K1 and K10 represent early differentiation markers, whereas IVL or transglutaminase I are late markers of keratinocyte differentiation. Using RT-PCR, we analyzed early and late differentiation markers in HaCaT (Fig. 1C) and hPK (Fig. 1D) cells. As shown in Fig. 1C low K1, K10, as well as IVL and TGM1 mRNA concentrations were detected in medium containing

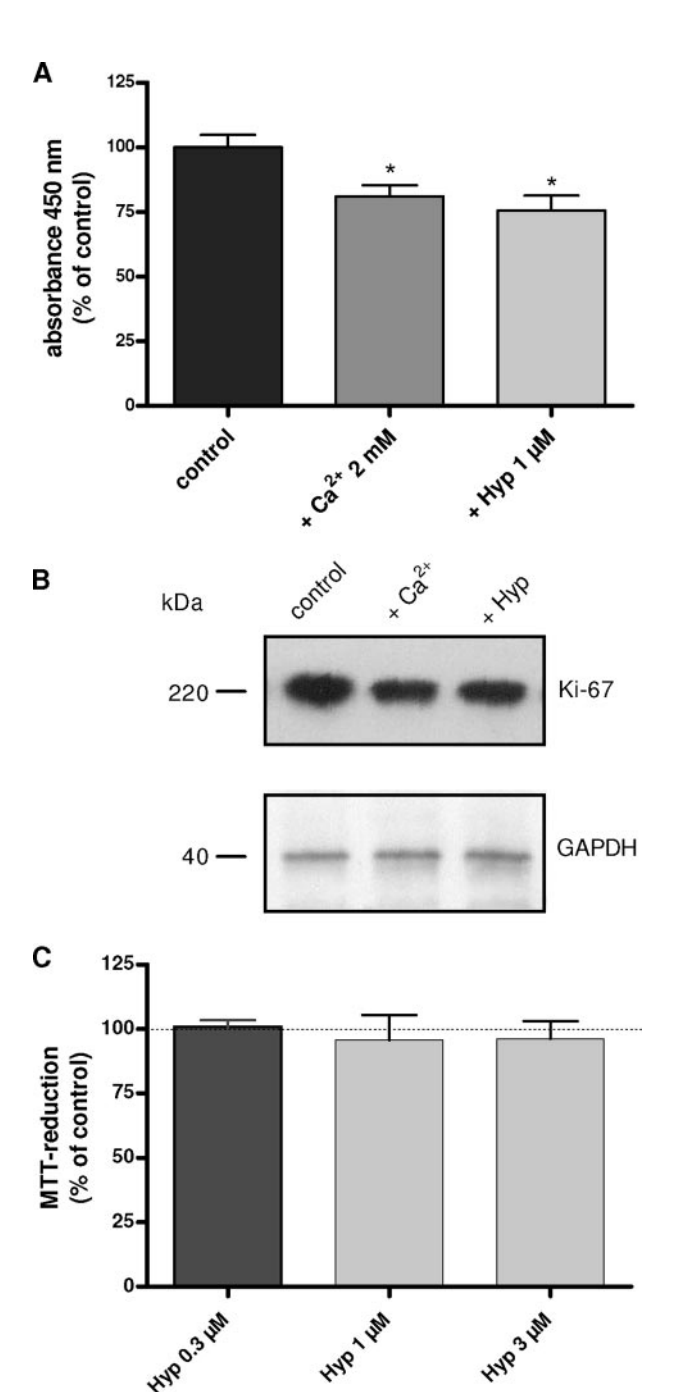


FIGURE 2. **Hyperforin inhibits proliferation in HaCaT keratinocytes.** HaCaT keratinocytes were incubated for 3 days with Ca<sup>2+</sup> (2 mm) or hyperforin (*Hyp*, 1  $\mu$ m). *A*, the proliferation measurement in synchronized HaCaT cells was performed with the bromodeoxyuridine immunoassay kit (Calbiochem), according to the manufacturers instructions. Synchronization was achieved by 24 h serum withdrawn. The relative changes in percentage in the absorbance at 450 nm compared with the untreated control were measured (n=3; \*, p<0.1, unpaired t test). *B*, Western blotting of Ki-67 in protein samples taken from untreated (control) or treated HaCaT cells, compared with GAPDH. Shown is a representative blot from a single experiment that was repeated three times. *C*, HaCaT cells were treated with hyperforin at different concentrations (0.3–3  $\mu$ m) for 48 h. The relative changes in percentage in the MTT reduction compared with the untreated control were measured (n=3).

0.1 mM  ${\rm Ca^{2}}^{+}$ , whereas their mRNA levels were increased in cells cultured in the presence of either high  $[{\rm Ca^{2}}^{+}]_{o}$  or hyperforin. Quantification of the RT-PCR signals obtained from mRNA extracted from HaCaT (Fig. 1*E*) and hPKs (Fig. 1*F*) by



normalization clearly show that incubation in the presence of high [Ca<sup>2+</sup>]<sub>a</sub> as well as hyperforin increased the transcription of early and late keratinocyte differentiation markers.

Hyperforin Inhibits Proliferation in HaCaT Keratinocytes— In addition to differentiation, proliferation of keratinocytes is also controlled by intracellular free Ca<sup>2+</sup> concentration. There-

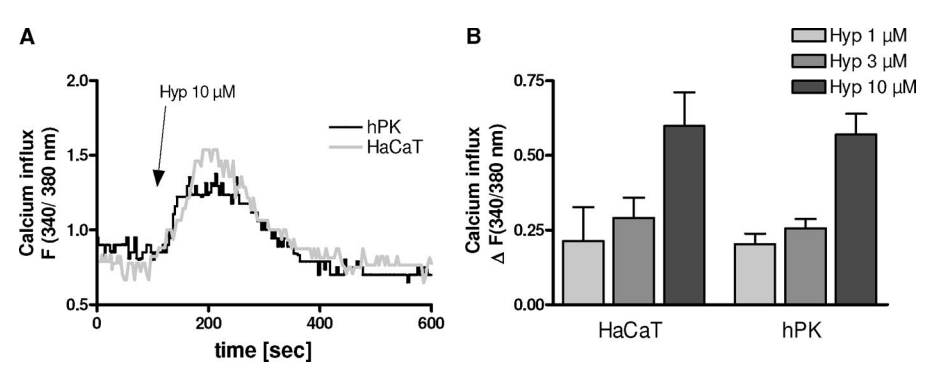


FIGURE 3. Hyperforin induces nonselective cation influx in HaCaT keratinocytes. A, representative time traces show hyperforin-induced changes in [Ca<sup>2+</sup>], in fura-2-loaded HaCaT and hPK cells. Hyperforin (*Hyp*, 10 μM) was added 50 s after the start of the experiment. B, HaCaT cells and hPKs were stimulated with various concentration of hyperforin (n = 6).

fore, we performed proliferation measurements with the bromodeoxyuridine immunoassay kit (Chemicon). Synchronized HaCaT keratinocytes incubated with high [Ca<sup>2+</sup>]<sub>a</sub> for 3 days showed significantly reduced proliferation (Fig. 2A). Notably, hyperforin (1  $\mu$ M) also inhibited the proliferation of keratinocytes, as shown in Fig. 2A. To confirm these findings, we ana-

> lyzed the expression of the nuclear proliferation marker protein Ki-67 by Western blotting. Ki-67 is expressed in cells undergoing the S/G<sub>2</sub>/M transition and serves as a well established marker to determine proliferating cells (21). As shown in Fig. 2B, protein expression of Ki-67 is similarly reduced in HaCaT cells treated either with hyperforin or high  $[Ca^{2+}]_o$ . To exclude toxic effects induced by hyperforin, we performed MTT assay (Fig. 2C). The test showed clearly that hyperforin had no influ-

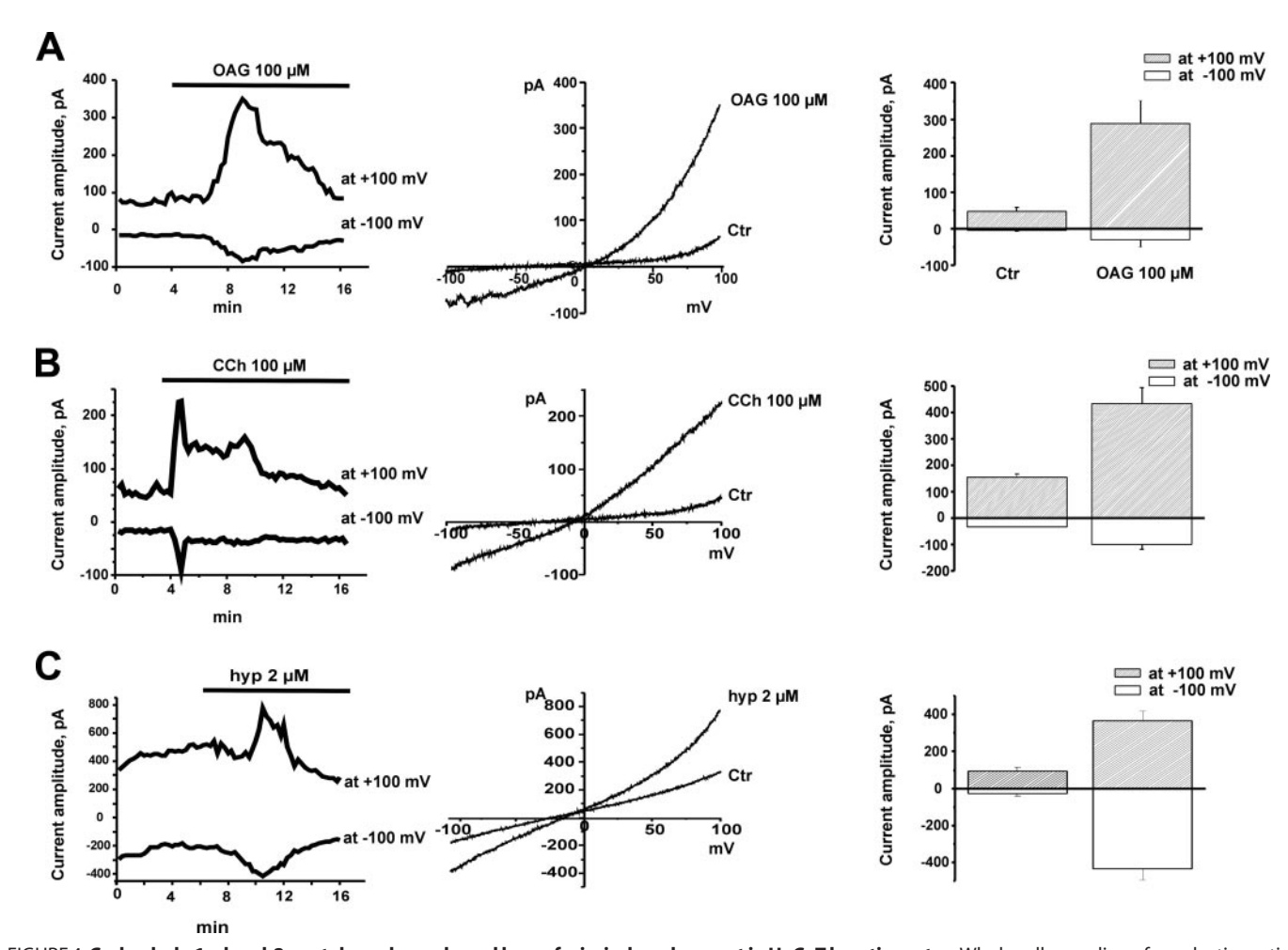


FIGURE 4. Carbachol-, 1-oleoyl-2-acetyl-sn-glycerol-, and hyperforin-induced current in HaCaT keratinocytes. Whole cell recording of unselective cation currents in HaCaT cells were obtained in response to 1-oleoyl-2-acetyl-sn-glycerol (OAG, A), carbachol (CCh, B), and hyperforin (hyp, C). The data are gathered from voltage ramp from -100 to +100 mV. Left panels, currents measured at -100 and +100 mV are plotted over time. The presence of the drugs is shown by horizontal bars. Middle panels, shown are the corresponding I-V relationships of the cells in the left panels measured before and during maximal agonist response. Right panels, the mean current amplitudes are presented as bars (n=8 for 100  $\mu$ M 1-oleoyl-2-acetyl-sn-glycerol, n=6 for 100  $\mu$ M carbachol, n=13for 2–10  $\mu$ M hyperforin). Ctr, control.



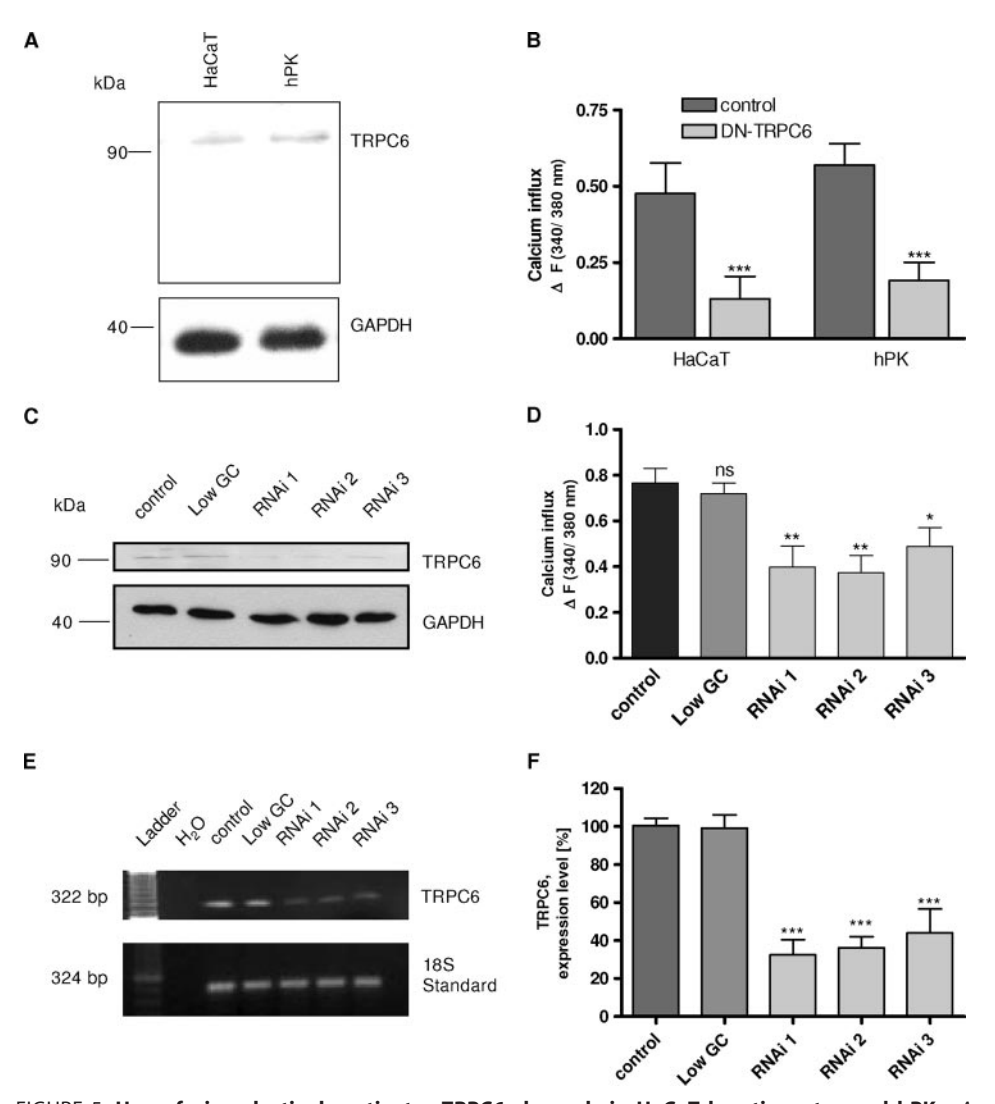


FIGURE 5. Hyperforin selectively activates TRPC6 channels in HaCaT keratinocytes and hPKs. A, Western blotting of HaCaT cells and hPKs confirms the presence of TRPC6 channel protein in both cell types. B, HaCaT cells and hPKs were transfected with TRPC6-DN-YFP. 48 h after transfection, the cells were loaded with fura-2-AM and were stimulated with hyperforin. The asterisks denote statistical significance as compared with untransfected keratinocytes (n=12,5-10 cells/independent experiment; \*\*\*, p<0.001, unpaired t test). C, we analyzed HaCaT keratinocytes transfected with control as well as three different anti-TRPC6 siRNAs abbreviated with RNAi 1-3. Because GC content of the anti-TRPC6 siRNAs, we used a random RNAi with low GC content to control RNAi 1-3. RNAi-transfected HaCaT cells were analyzed by Western blot using anti-GAPDH and anti-TRPC6 antibodies. Staining with an anti-TRPC6 antibody resulted in a single band with a molecular mass of around 97 kDa. D, HaCaT cells were transfected with anti-TRPC6 RNAis (RNAi 1, 2, and 3) and control RNAi with low GC content (Low GC). In addition, untransfected cells were used as additional control. After an incubation period of 48 h, HaCaT cells were loaded with fura-2 and were stimulated with hyperforin (10  $\mu$ M) (n=6, 5–10 cells/independent experiment. \*\*\*, p<0.001, unpaired t test; ns, nonsignificant. E, the effectiveness of RNAi transfection was determined in RT-PCR analyses. F, histogram reflecting relative expressing level of TRPC6, normalized to its expression level in untransfected control cells. The asterisks denote statistical significance as compared with control HaCaT keratinocytes (n = 3; \*\*\*, p < 0.001, unpaired t test).

ence on cell viability at the concentrations used for the differentiation experiments. These findings show that the anti-proliferative effect of hyperforin in keratinocytes was not due to the toxicity of the substance.

Hyperforin Induces Ca<sup>2+</sup> Influx in HaCaT Keratinocytes and hPK via TRPC6—Because we detected TRPC6 expression in keratinocytes via RT-PCR prior to our approach using hyperforin as specific pharmacological tool to mimic TRPC6-mediated effects, we studied functional hyperforin-mediated changes in intracellular calcium (Fig. 3) and transmembrane

currents in keratinocytes (Fig. 4). As shown in Fig. 3A, hyperforin (10 μM) reproducibly induced rapid and transiently elevations of calcium-dependent fluorescence in fura-2-loaded HaCaT keratinocytes and in hPKs. The response was suppressed in the presence of Ca<sup>2+</sup>-free measuring buffer (supplemental Fig. S1), indicating that the hyperforin-induced effect is mainly mediated by an influx across the plasma membrane. The hyperforin-mediated changes in fluorescence were concentration-dependent, and even at low concentrations (1 μM) significant elevations were reproducibly detectable (Fig. 3B). For further characterization, we substituted calcium in the buffer by barium or strontium ions, resulting in enhanced fluorescence upon the application of hyperforin (supplemental Fig. S1). In addition, the hyperforin-mediated changes in fluorescence were suppressed in the presence of several compounds (gadolinum chloride, lanthanum chloride, SK&F 96365, 2-aminophenoxyborate, and N-(p-amylcinnamoyl) anthranilic acid) described as unselective TRPC channel blockers (supplemental Fig. S1). Because we wanted to know whether hyperforin can stimulate endogenous ion channels expressed in the HaCaT keratinocyte cell line, we conducted whole cell patch clamp experiments using the perforated patch configuration. As illustrated in Fig. 4, activation of unselective cation channel currents was observed by 100 µM 1-oleoyl-2-acetyl-sn-glycerol in 8 of 10 HaCaT cells (Fig. 4A), by 100  $\mu$ M carbachol in 6 of 10 cells (Fig. 4B), and by 2  $\mu$ M hyperforin in 13 of 14 cells (Fig. 4C). The reversal potential of the induced currents were

 $0.5\pm3.4$ ,  $-12.3\pm4.9$ , and  $0.7\pm3.0$  mV, respectively. Pretreatment of the cells by  $100~\mu{\rm M}~{\rm Gd}^{3+}$  blocked the hyperforin induced current amplitude by  $74\pm11\%~(n=5)$ . The elicited conductance showed slight outward rectifications.

Because the functional features measured in keratinocytes strongly suggested that the hyperforin-stimulated effects are mediated by TRPC6, we analyzed protein extract of keratinocytes by Western blots. Using a commercially available anti-TRPC6 antibody, we were able to detect a protein with the appropriate molecular mass in membrane extracts of HaCaT



cells (Fig. 5A, left lane) as well as hPKs (Fig. 5A, right lane). To validate that the hyperforin-induced changes in intracellular calcium are mediated by TRPC6, we studied the hyperforininduced Ca2+ entry in HaCaT cells and hPKs expressing a dominant negative TRPC6 mutant (Fig. 5B). HaCaT cells and hPKs were transfected with a TRPC6-YFP mutant with dominant negative character (TRPC6-DN-YFP) (22) for 2 days, and Ca<sup>2+</sup> influx was measured. In transfected HaCaT keratinocytes and hPKs selected by the YFP fluorescence, hyperforin-induced  $Ca^{2+}$  influx was significantly reduced (Fig. 5B). Because the knockdown approach using dominant negative TRPC mutants is based on multimerization of TRPC channel subunits, this approach is handicapped by the promiscuous interaction of TRPC channel within specific subgroups (here TRPC3, TRPC6, and TRPC7). To further evaluate whether or not TRPC6 is involved in keratinocyte differentiation, we induced specific knockdown of TRPC6 via transfection of HaCaT cells with siRNAs directed against TRPC6 (Fig. 5, C and D). Western blot analyses were used for optimization of experimental conditions and to analyze TRPC6 protein expression. In preparations of HaCaT cells transfected with anti-TRPC6 RNAi 1 and 2, the protein levels were drastically reduced, whereas in HaCaTs transfected with RNAi 3 TRPC6 protein was reduced but still detectable (Fig. 5C). In control siRNA-transfected keratinocytes, TRPC6 protein was unchanged; strong bands with appropriate molecular mass were detectable. The RT-PCR analyses (Fig. 5, E and F) of TRPC6 siRNA transfected cells reflect the Western blot findings, demonstrating the effectiveness of the siRNA experiments. Additionally, we studied hyperforin-induced changes in calcium-dependent fluorescence in HaCaT cells transfected with anti-TRPC6 RNAi 1-3 (Fig. 5D). The hyperforin-induced Ca2+ entry was not affected in control siRNA transfected cells. In contrast, the increase in Ca<sup>2+</sup> was significantly diminished in keratinocytes transfected with anti-TRPC6 RNAi 1-3. Like expected from the Western blot analysis and RT-PCR experiments, in anti-TRCP6 RNAi 3 transfected cells, hyperforin-induced Ca<sup>2+</sup> influx was higher than in RNAi 1 and 2.

Role of TRPC6 Channels in hPK and Human Skin Explants ex Vivo-To evaluate the role of TRPC6 in situ, we performed cytospins with hPKs and incubated living skin with the endogenous stimulus Ca2+ (2 mm) and hyperforin ex vivo. As shown in Fig. 6, Ca<sup>2+</sup> and hyperforin induced the expression of TRPC6 in hPKs to a similar extent as  $Ca^{2+}$  (2 mM) (Fig. 6A, panels a-c). Similarly, both Ca2+ and hyperforin induced a significant increase of TRPC6 expression in short term cultured human skin explants (Fig. 6A, panels d and e, and B and C). In both models, TRPC6 positive keratinocytes showed staining of the cell membrane and the cytoplasm. In the skin explants, TRPC6 was primarily expressed by stratum spinosum and stratum granulosum keratinocytes (Fig. 6A, panels e and f). In contrast, basal keratinocytes were negative for TRPC6 (Fig. 6C), indicating that only keratinocytes entering the epidermal differentiation process are susceptible for TRPC6 expression. Interestingly, there was a lamellar accumulation of TRPC6 reactivity in the distal stratum granulosum where keratinocytes physiologically flatten, dissolve their nucleus, and disintegrate during their terminal differentiation (Fig. 6A, panels e and f). Positive

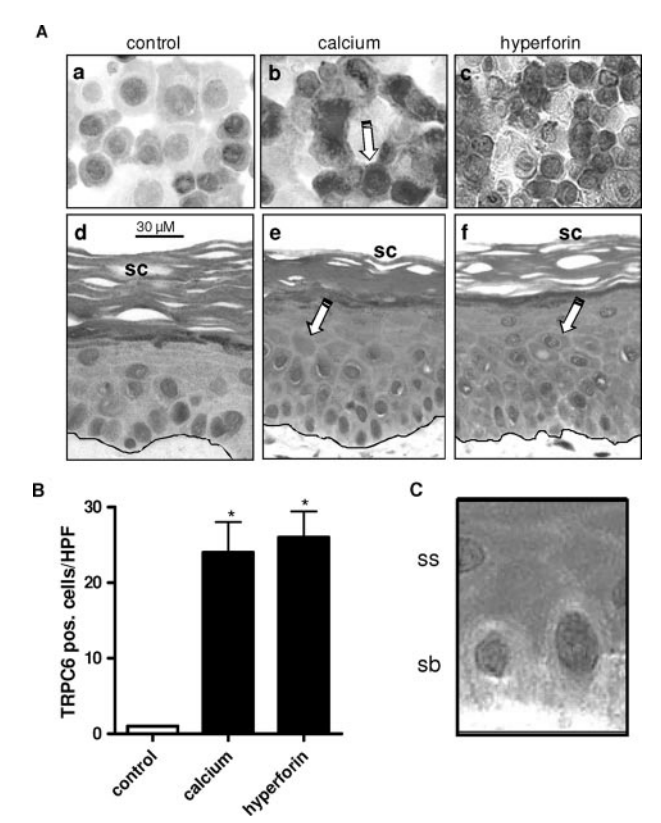


FIGURE 6. Hyperforin induces TRPC6 expression in human hPKs in vitro (A, panels a-c) and in living human skin ex vivo (A, panels d-f, and B and C). A, panels a-c, hPKs were incubated for 24 h in Ca<sup>2+</sup>-free medium (control), 2 mm  $Ca^{2+}$  (positive control), or 1  $\mu$ m hyperforin. After centrifugation onto cytospin slides, the cells were stained for TRPC6 expression (red staining, see arrow). Representative images (×400 magnification) from four independent experiments are shown. A, panels d-f, and B and C, split thickness skin organ culture. Skin explants obtained from dermatome-separated human skin were incubated for 24 h in Ca<sup>2+</sup>-free medium (control), 2 mm Ca<sup>2+</sup> (positive control), or 1  $\mu$ M hyperforin. 3- $\mu$ m sections were stained for TRPC6 (red staining). Representative sections of high power fields are shown in A, panels d-f. The arrows indicate TRPC6-positive cells. Positive staining of the stratum corneum (sc) indicates accumulation of TRPC6 protein in the keratin envelope of the epidermis. Five random fields of sections from four independent skin explants were counted for TRPC6-positive keratinocytes at ×400 magnification. The final count/group represents the mean  $\pm$  S.D. B, \*, p < 0.05. Note the absence of TRPC6 expression in stratum basale (sb) keratinocytes but strong positivity of stratum spinulosum (ss) keratinocytes as illustrated in a detail from Ca<sup>2+</sup>-treated skin (C).

staining of the stratum corneum indicates that TRPC protein is not degraded but integrated in the keratin envelope of the epidermis (Fig. 6A, panels d-f).

TRPC6 Activation Mediates the Hyperforin-induced Differentiation—After having shown that the hyperforin-induced changes in intracellular calcium concentrations are mediated by TRPC6 expressed in keratinocytes, it was fascinating to test whether hyperforin-induced differentiation in HaCaT keratinocytes is based on TRPC6 expression as well. We addressed this question by analyzing morphology of hyperforin-treated siRNA-transfected cells (Fig. 7A) or in cells after expression of dominant negative TRPC6 (Fig. 7B). Keratinocytes transfected with control siRNA showed typical differentiated-related morphology when treated with hyperforin (1  $\mu$ M), whereas HaCaT cells transfected with RNAi 1-3 were morphologically unchanged after incubation for 3 days in the presence of 1  $\mu$ M hyperforin (Fig. 7A). Like siRNA transfection, transfection with



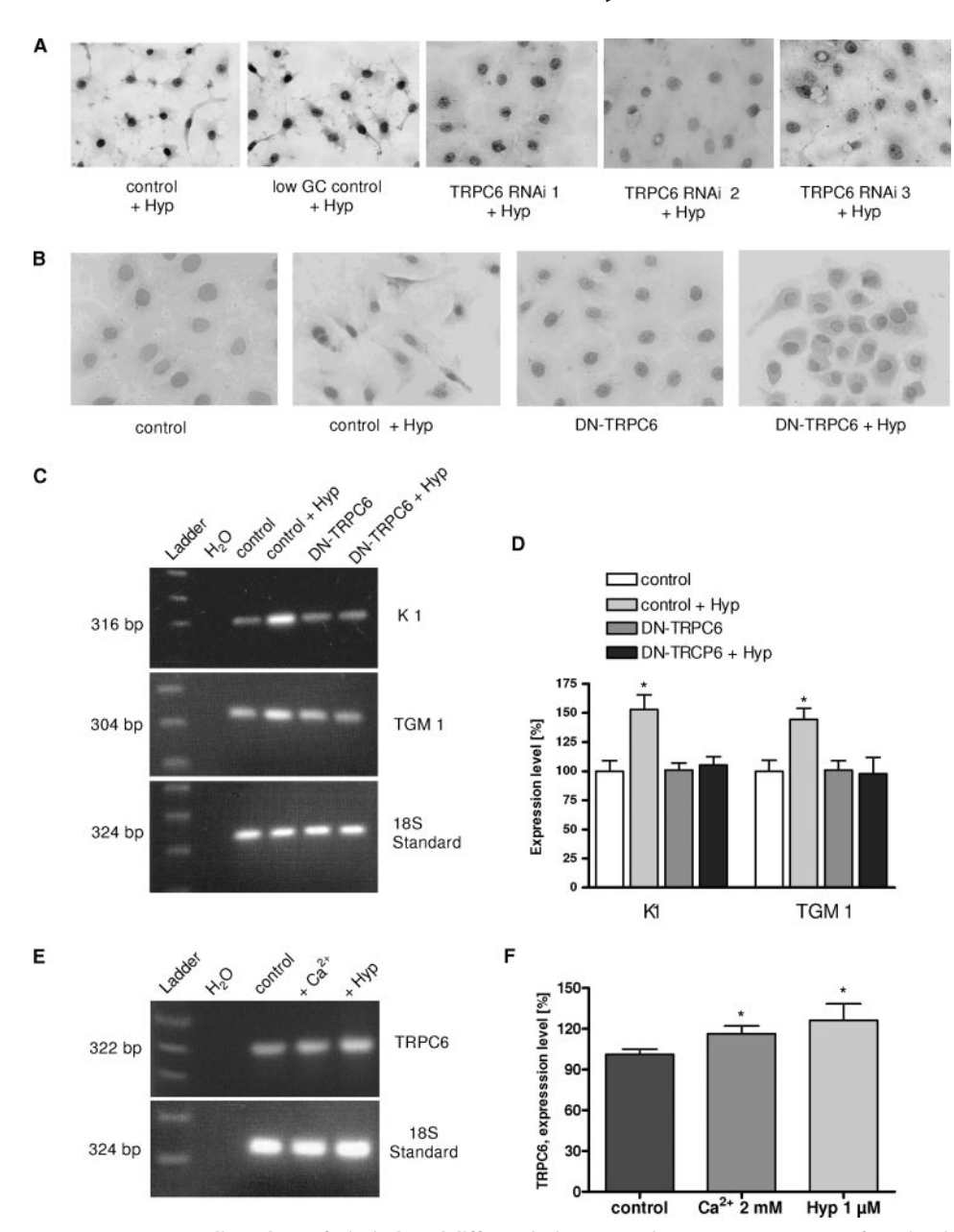


FIGURE 7. **TRPC6 mediates hyperforin-induced differentiation.** HaCaT keratinocytes were transfected with TRPC6-DN, anti-TRCP6 RNAis, or control RNAi with low GC content and incubated for 3 days with hyperforin (Hyp, 1  $\mu$ M). A, anti-TRPC6 RNAis and RNAi control transfected HaCaT cells were incubated for 3 days with hyperforin (1  $\mu$ M) and stained with Mayer's hematoxylin and eosin solutions. Representative images demonstrate how TRPC6 silencing affects the hyperforin-induced morphology changes. B, keratinocytes were stained with Mayer's hematoxylin and eosin solutions. Representative images of untransfected or DN-TRPC6-transfected HaCaT cells treated with hyperforin (1  $\mu$ M) are shown from at least three experiments. C, expression of differentiation markers in untreated (untransfected and DN-TRPC6 transfected) HaCaT cells and hyperforintreated (1  $\mu$ M) (untransfected or DN-TRPC6 transfected) cells was determined in RT-PCR analysis. D, histogram reflecting relative expressing levels of differentiation markers, compared with their normalized expression levels in untransfected, untreated HaCaT cells. The asterisks denote statistical significance as compared with control HaCaT keratinocytes (n = 3;\*, p < 0.1, unpaired t test). E, HaCaT keratinocytes were incubated for 3 days with calcium (2 mM) and hyperforin (1  $\mu$ M). Total mRNA was isolated, reverse transcribed, and subjected to PCR. Expression of TRPC6 was detected. F, histogram reflecting the quantitative changes in TRPC6 expression following Ca<sup>2+</sup>- and hyperforin-induced differentiation (n = 3).

the plasmid coding for a dominant negative TRPC6 variant suppressed hyperforin-induced morphological changes (Fig. 7*B*). In addition to morphological changes, we examined the mRNA levels of the early differentiation marker K1 and the late differentiation marker TGM I in DN-TRPC6 transfected and untransfected HaCaT keratinocytes (Fig. 7, *C* and *D*). As

already shown, K1 and TGM I mRNA level were increased in non-transfected cells treated with hyperforin (compare Fig. 1, *B*–*F*, with Fig. 7, *C* and *D*). Remarkably, hyperforin had no effect on the expression of both differentiation markers in DN-TRPC6 transfected keratinocytes (Fig. 7*D*).

As a next step, we examined the expression of TRPC6 channels in HaCaT keratinocytes under control (low Ca<sup>2+</sup>) and differentiating (high [Ca<sup>2+</sup>]<sub>o</sub> or hyperforin) conditions. For this, we analyzed the mRNA levels of the channel protein in cells treated for 2 days with Ca<sup>2+</sup> (2 mm) and hyperforin (1  $\mu$ M), compared with untreated control cells. The data showed that TRPC6 mRNA levels in human keratinocytes are slightly increased after incubation with high [Ca2+], (Fig. 7E). Similarly, we observed a significant increase in TRPC6 transcripts in HaCaT keratinocytes, kept in hyperforin-containing medium for 2 days (Fig. 7F). Overall these data are in accordance with reports published earlier (12).

TRPC6 Channels Are Involved in High  $[Ca^{2+}]_o$ -mediated  $Ca^{2+}$  Influx and Differentiation—With our new findings in mind, we subsequently investigated the role of TRPC6 channels for high [Ca<sup>2+</sup>]<sub>a</sub>-induced Ca2+ influx and differentiation. In line with published findings (20, 23), we were able to measure changes in calcium-dependent fluorescence in response to acutely applied high [Ca<sup>2+</sup>]<sub>o</sub> in HaCaT keratinocytes (Fig. 8A). To determine whether the high [Ca<sup>2+</sup>]<sub>a</sub>-induced responses monitored in keratinocytes (Fig. 1) are mediated by TRPC6 channels, we transfected cells with siRNAs directed against TRPC6 and analyzed calcium homeostasis, morphology, and expression level of marker proteins (Fig. 8, B-E). The results show that in cells transfected

with anti-TRPC6RNAihigh[Ca²+] $_o$ -induced changesincalcium-dependent fluorescence were reduced (Fig. 8B). Keratino cytes transfected with control siRNA showed typical differentiated related morphology when treated with high [Ca²+] $_o$ , whereas HaCaT cells transfected with RNAi 1–3 were morphologically unchanged (Fig. 8C). The cell shape was affected by TRPC6



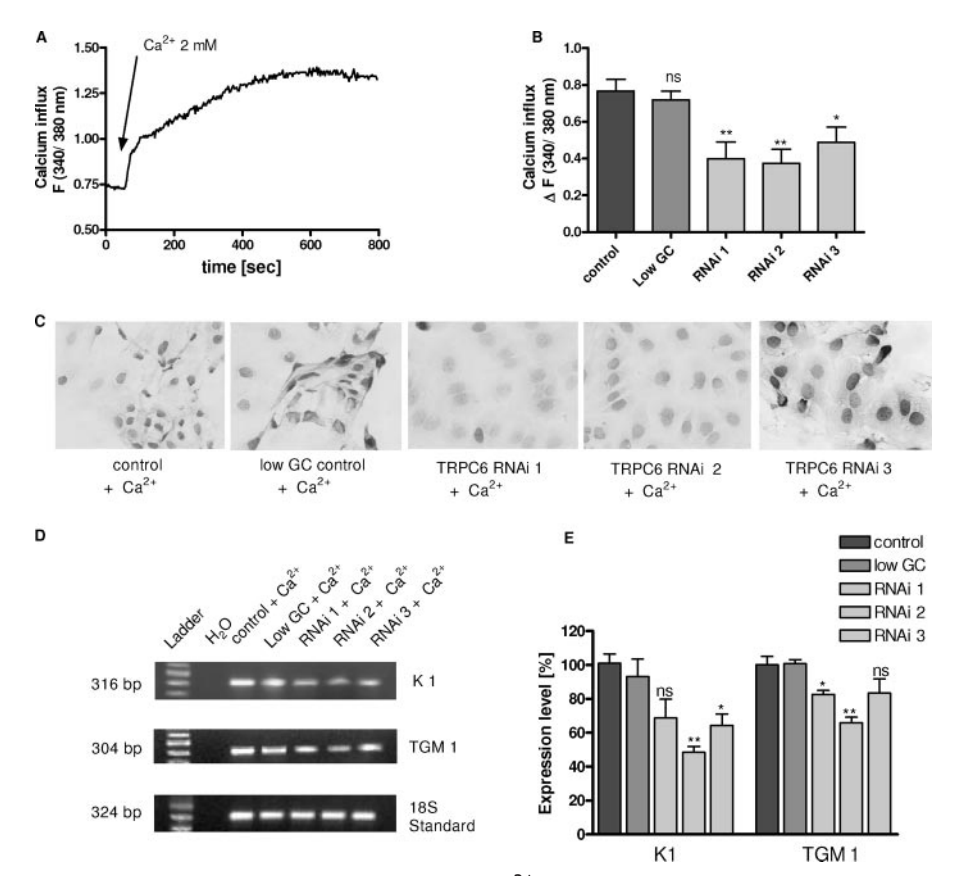


FIGURE 8. TRCP6 is involved in the high extracellular Ca<sup>2+</sup> concentration-induced differentiation. A, representative time traces show high extracellular Ca<sup>2+</sup>-induced changes in [Ca<sup>2+</sup>], in fura-2-loaded HaCaT cells. (2 mm) was added 50 s after start of experiment. B, HaCaT cells were transfected with anti-TRPC6 RNAis (RNAi 1, 2, and 3) and control RNAi with low GC content (Low GC). In addition, untransfected cells were used as additional control. After an incubation period of 48 h, HaCaT cells were loaded with fura-2 and were stimulated with Ca<sup>2+</sup> (2 mm) (n = 6, 5–10 cells/independent experiment; \*, p < 0.1; \*\*, p < 0.01, unpaired t test; ns, nonsignificant). C, anti-TRPC6 RNAis and RNAi control transfected HaCaT cells were incubated for 3 days with Ca<sup>2+</sup> (2 mm) and stained with Mayer's hematoxylin and eosin solutions. Representative images demonstrate how TRPC6 silencing affects the high extracellular Ca<sup>2+</sup>-induced morphology changes. *D*, expression of differentiation markers in anti-TRPC6 RNAis (RNAi 1, 2, and 3), control RNAi-transfected and untransfected HaCaT cells was determined in RT-PCR analysis. HaCaT cells were incubated for 3 days with Ca<sup>2+</sup> (2 mm). E, histogram reflecting relative expressing levels of differentiation markers, compared with their normalized expression levels in untransfected, untreated HaCaT cells. The asterisks denote statistical significance as compared with control HaCaT keratinocytes (n = 3; \*, p < 0.1; \*\*, p < 0.01 unpaired t test).

silencing, preventing the transformation of the cells from well rounded to flattened form allowing assembling monolith layer. Finally in anti-TRCP6 RNAi 1-3 transfected cells, the mRNA levels of differentiation markers were decreased, compared with expression levels of untransfected HaCaT cells treated with high  $[Ca^{2+}]_o$  (Fig. 8, D and E).

The Contribution of other TRPC Channels to Calcium- and Hyperforin-induced Effects in Keratinocytes—To investigate the role of other TRPC channels, we also knocked down TRPC1, TRPC3, TRPC4, TRPC5, and TRPC7 using the siRNA technique (Fig. 9). The effectiveness of silencing the expression was determined in RT-PCR analyses (Fig. 9, C and D). Only the silencing of TRPC6 diminished the hyperforin-induced calcium influx (Fig. 9A), providing additional proof for the central role of TRPC6 channels in keratinocyte physiology. Furthermore, we tested the effect of TRPC knockdown on high [Ca<sup>2+</sup>]<sub>a</sub>-induced calcium influx. In contrast to the clear result of the hyperforin-induced calcium entry, the role of TRPC channels in high [Ca<sup>2+</sup>]<sub>a</sub>-induced calcium influx is much more complex. As shown in Fig. 9B, TRPC1, TRPC3, TRPC4, and TRPC6 knockdown significantly reduced the calcium influx, whereas TRPC5 and TRPC7 silencing had no significant effect on the calcium influx upon [Ca<sup>2+</sup>]<sub>a</sub> elevation.

#### **DISCUSSION**

Hyperforin, the specific TRPC6 activator, allowed us to study for the first time the specific role of TRPC6 channels in keratinocyte differentiation. We used two different cell models, HaCaT and hPK cells and human skin explants as native systems. Based on RT-PCR analyses, a variety of TRPC channel combinations have been identified in human keratinocytes in literature (12, 13). Beck et al. (13) detected no TRPC6 or TRPC3 channels but TRPC1, TRPC4, TRPC5 and TRPC7 channels. In contrast, Cai et al. (12) found TRPC1, TRPC3, TRPC4, TRPC5, and TRPC6 channels by RT-PCR analysis. The controversial results made it indispensable to analyze TRPC channels in the cells used for further experiments. Western blot and RT-PCR analyses showed TRPC6 channel expression in HaCaTs and hPK cells. The biochemical data were validated by the functional approaches calcium imaging, patch clamp experiments in hPKs and HaCaT cells. In both cell models, hyperforin induced a rapid and robust calcium influx,

which could be inhibited by several TRP channel blockers like SK&F 96365, N-(p-amylcinnamoyl) anthranilic acid, 2-aminophenoxyborate, La<sup>3+</sup>, or Gd<sup>3+</sup>. In addition to calcium influx, we also found a nonselective cation influx of Ba<sup>2+</sup> and Sr<sup>2+</sup> ions in hPK and HaCaT cells. Patch clamp recordings showed a robust hyperforin-dependent activation of an unselective cation channel in HaCaT cells. The shape of the current-voltage relationship was comparable with data already described for heterologously expressed TRPC6 (16). The hyperforin-induced currents were blocked by gadolinium as reported previously for heterologously expressed TRPC6 (16). Based on the fact that the RT-PCR analyses of the HaCaT cells used resulted in a broad profile of expressed TRPC channels, we finally decided to knock down all TRPC channels in parallel experimental set ups. This broad approach clearly showed that the hyperforin-mediated effect in HaCaT cells were mediated by TRPC6.

In addition to the acute effects on intracellular ion concentration, hyperforin is also inducing differentiation in HaCaT and hPK cells via TRPC6 channels. Disturbed keratinocyte dif-



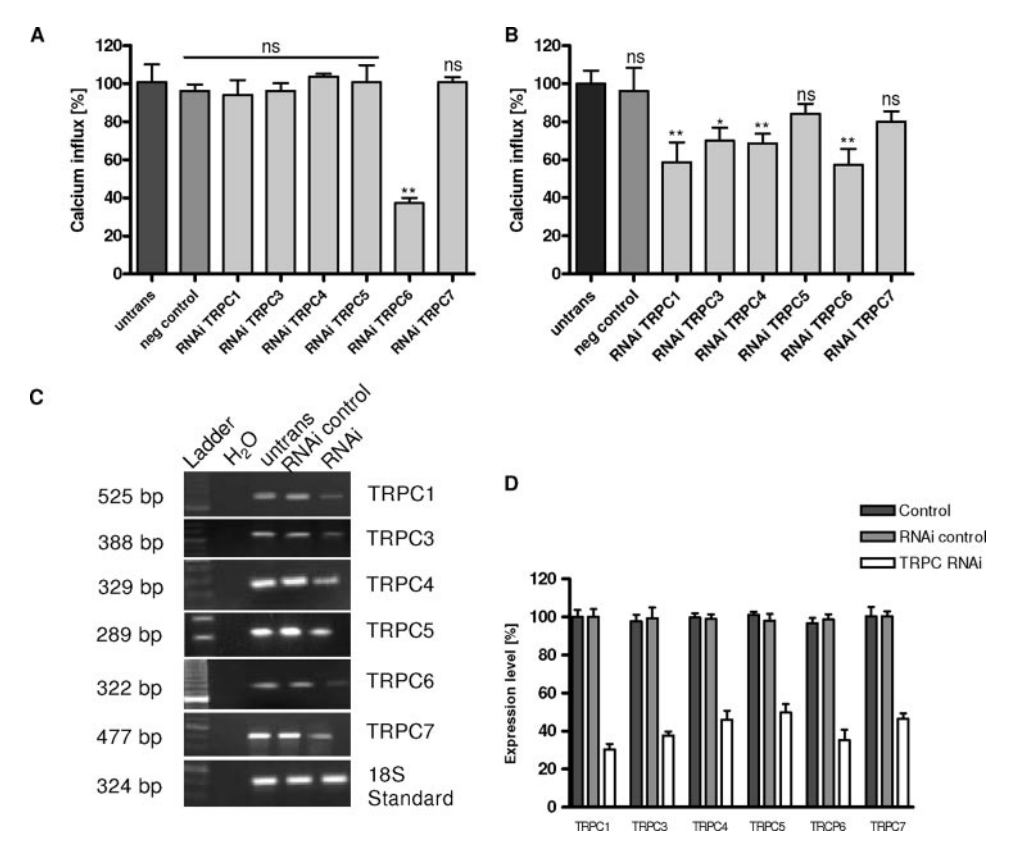


FIGURE 9. Role of other TRPC channels in hyperforin- and high calcium-induced effects in keratinocytes. HaCaT keratinocytes were transfected with control siRNA and the respective siRNA for every TRPC channel. After an incubation period of 48 h, HaCaT cells were loaded with fura-2 and were stimulated with hyperforin (A) or Ca<sup>2+</sup> 2 mM (B) (n=6; \*, p<0.1; \*\*, p<0.01, unpaired t test; ns, nonsignificant). C, the effectiveness of the respective RNAi transfection was analyzed in RT-PCR experiments. D, histogram showing the relative expression of the TRPC channels, compared with their normalized expression levels in untransfected, untreated HaCaT cells (n=3).

ferentiation and proliferation have been detected in several skin diseases like AD and psoriasis (5). Several TRPC channels including TRPC6 are discussed as playing a major role for the Ca<sup>2+</sup>-mediated regulation of keratinocyte differentiation (12). However, investigating their individual role was hampered by the lack of specific stimulation or inhibitors. Because we have recently identified hyperforin as a specific and potent TRPC6 activator (16), the aim of our present study was to investigate the contribution of TRPC6 for differentiation and proliferation of human keratinocytes using hyperforin as tool to specifically activate these channels. Our findings clearly show that hyperforin induces Ca<sup>2+</sup> influx via the activation of TRPC6 channels in both hPK and HaCaT cell models. As has been shown, increasing [Ca<sup>2+</sup>], in keratinocytes resulted in augmented expression of several differentiation markers (1, 20). Elevated [Ca<sup>2+</sup>], evoked by hyperforin also led to an enhanced expression of cytokeratins K1 and K10 and late differentiation markers, e.g. TGM1 or IVL in human keratinocytes. TRPC6 knockdown by two different approaches, namely siRNA technique and transfection with a dominant negative TRPC6 mutant, inhibited hyperforin-mediated differentiation, further confirming that TRPC6 is essential for the hyperforin-induced differentiation. TRPC6 knockdown by transfection with the TRPC6 mutant also inhibited the expression of K1 and transglutaminase I, crucial components required for keratinocyte differentiation. Moreover, TRPC6 expression pattern is linked to the differentiation state influenced by hyperforin or Ca2+. Furthermore, we proved the ex vivo relevance of TRPC6 channels in human skin explants. Ca2+ and hyperforin induced to a similar extent the expression of TRPC6 in hPKs and in short term cultured human skin explants. In the skin explants, TRPC6 was primarily expressed by stratum spinosum and stratum granulosum keratinocytes and not in basal keratinocytes, supporting our findings that keratinocyte epidermal differentiation depends on TRPC6 expression.

Role of TRPC Channels in Keratinocyte Differentiation—Because their expression levels change in a differentiation-dependent manner, functional properties of TRPC channels in keratinocytes have been suggested to be involved in differentiation, which is regulated by Ca<sup>2+</sup> influx (12, 14, 15). Recently, TRPC1 has been implicated in the Ca<sup>2+</sup>-induced terminal differentiation of human keratinocytes in vitro (14, 24). However, silencing TRPC1 did not completely block keratinocyte differentiation, suggesting that

other TRPC channels may also be involved, particularly because they are known to form multimers in vivo. TRPC4 and TRPV6 have also been reported to take part in keratinocyte differentiation (15, 25). Our results about the involvement of TRPC1, TRPC3, TRPC4, and TRPC6 in the high [Ca<sup>2+</sup>]<sub>o</sub>-induced effects confirm these data. But our finding about the involvement of TRPC6 in the Ca2+- and hyperforin-induced differentiation identifies a new key player in keratinocyte differentiation. Even if other TRPC or TRPV channels might be involved in keratinocyte differentiation, our findings of nearly similar differentiation responses following high [Ca<sup>2+</sup>] or by the specific TRPC6 activator hyperforin suggest that TRPC6 activation alone is sufficient for full physiological response and that TRPC6 plays a fundamental role for the regulation of keratinocyte differentiation by high [Ca<sup>2+</sup>]<sub>a</sub>. However, although TRPC6 expression, regulation, and functions in brain (26) and kidney (27) have been previously studied, the role of TRPC6 in the epidermis, where Ca<sup>2+</sup> plays a fundamental role in cell physiopathology, was not elucidated until now. We suggest that up-regulation of the TRPC6 channels in differentiated cells is an important contributory component in Ca<sup>2+</sup> entry, thereby promoting differentiation. Modulation of TRPC6, such as stimulation with hyperforin, might therefore be a potential treatment for correcting the disturbed differentiation in skin diseases.



Differentiation and Proliferation Defects in Skin Pathophysiology-Many studies demonstrate the existence of a steep Ca<sup>2+</sup> gradient in the human epidermis (28, 29). This Ca<sup>2+</sup> gradient seems to play an important role in the regulation of epidermal function. First, the formation of the Ca<sup>2+</sup> gradient coincides with key steps of barrier formation and stratum corneum development (30). Second, skin diseases characterized by an abnormal barrier, such as AD and psoriasis, are accompanied by a loss of the Ca2+ gradient (31, 32). Proksch and co-workers (6) reported that impaired differentiation is involved in the defective barrier function found in AD and that the disturbance in barrier function enables aeroallergens to penetrate the skin more easily. In fact, a reduced amount of IVL in AD and K10 in lesional AD could be detected (5). Moreover, all of the psoriatic suprabasal cell layers displayed higher than normal concentrations of Ca<sup>2+</sup>, indicating loss of the normal Ca<sup>2+</sup> gradient that programs terminal differentiation (31). In addition to differentiation, proliferation also regulates skin barrier function. Actually, increased proliferation is often accompanied by disturbed differentiation (5), and an increased epidermal proliferation was detected in psoriasis and AD (2, 6). Again, Ca<sup>2+</sup> plays a regulatory role in keratinocyte proliferation. Not unexpectedly, Menon and Elias (31) observed that the basal layer of psoriatic lesions contained less [Ca<sup>2+</sup>]<sub>o</sub>, a condition that favored enhanced proliferation. Correcting these defects related to the permeability barrier and the Ca<sup>2+</sup> gradient is part of the therapeutic effect of occlusive dressings in psoriasis (33). Our data provide the rationale to use activation of TRPC6 channels by hyperforin or similar compounds as alternative treatment approach, because low concentrations of hyperforin are sufficient to obtain effects on keratinocyte differentiation similar to the effects that can be obtained by elevating the extracellular [Ca<sup>2+</sup>]<sub>o</sub> in vitro.

Hyperforin represents the major active constituent of St. John's wort (34), which has been used traditionally for centuries to heal wounds, burns, and other skin lesions (35). However, controlled clinical data are missing. Only one placebo-controlled study using a low concentration of a hyperforin-containing cream proved the topical treatment effective in patients with mild to moderate AD (36). However, the mechanism of hyperforin-induced effects was not sufficiently understood. Hyperforin has long been known to possess antibacterial activity (37, 38) and to inhibit the growth of multi-resistant strains of Staphylococcus aureus (39). Although its antibacterial properties may contribute to the positive effects in treatment of AD, our data may give an additional, quite plausible explanation for a dermatological use of hyperforin that deserves further investigation.

#### REFERENCES

- 1. Yuspa, S. H., Kilkenny, A. E., Steinert, P. M., and Roop, D. R. (1989) J. Cell Biol. 109, 1207-1217
- 2. Lowes, M. A., Bowcock, A. M., and Krueger, J. G. (2007) Nature 445,
- 3. Bovenschen, H. J., Seyger, M. M., and Van De Kerkhof, P. C. (2005) Br. J. Dermatol. 153, 72-78
- 4. Williams, H. C. (2005) N. Engl. J. Med. 352, 2314-2324

- 5. Proksch, E., Folster-Holst, R., and Jensen, J. M. (2006) J. Dermatol. Sci. 43, 159 - 169
- 6. Jensen, J. M., Folster-Holst, R., Baranowsky, A., Schunck, M., Winoto-Morbach, S., Neumann, C., Schutze, S., and Proksch, E. (2004) J. Investig. Dermatol. 122, 1423-1431
- 7. Palmer, C. N., Irvine, A. D., Terron-Kwiatkowski, A., Zhao, Y., Liao, H., Lee, S. P., Goudie, D. R., Sandilands, A., Campbell, L. E., Smith, F. J., O'Regan, G. M., Watson, R. M., Cecil, J. E., Bale, S. J., Compton, J. G., DiGiovanna, J. J., Fleckman, P., Lewis-Jones, S., Arseculeratne, G., Sergeant, A., Munro, C. S., El Houate, B., McElreavey, K., Halkjaer, L. B., Bisgaard, H., Mukhopadhyay, S., and McLean, W. H. (2006) Nat. Genet.
- 8. Tu, C. L., Oda, Y., Komuves, L., and Bikle, D. D. (2004) Cell Calcium 35, 265 - 273
- 9. Eckert, R. L., Crish, J. F., and Robinson, N. A. (1997) Physiol. Rev. 77, 397 - 424
- 10. Tu, C. L., Chang, W., and Bikle, D. D. (2007) J. Investig. Dermatol. 127, 1074 - 1083
- 11. Hofmann, T., Obukhov, A. G., Schaefer, M., Harteneck, C., Gudermann, T., and Schultz, G. (1999) Nature 397, 259 – 263
- 12. Cai, S. W., Fatherazi, S., Presland, R. B., Belton, C. M., and Izutsu, K. T. (2005) J. Dermatol. Sci. 40, 21-28
- 13. Beck, B., Zholos, A., Sydorenko, V., Roudbaraki, M., Lehen'kyi, V., Bordat, P., Prevarskaya, N., and Skryma, R. (2006) J. Investig. Dermatol. 126, 1982-1993
- 14. Cai, S., Fatherazi, S., Presland, R. B., Belton, C. M., Roberts, F. A., Goodwin, P. C., Schubert, M. M., and Izutsu, K. T. (2006) Pflügers Arch. Eur. J. Physiol. 452, 43-52
- 15. Fatherazi, S., Presland, R. B., Belton, C. M., Goodwin, P., Al Qutub, M., Trbic, Z., Macdonald, G., Schubert, M. M., and Izutsu, K. T. (2007) Pflügers Arch. Eur. J. Physiol. 453, 879 – 889
- 16. Leuner, K., Kazanski, V., Müller, M., Essin, K., Henke, B., Gollasch, M., Harteneck, C., and Müller, W. E. (2007) FASEB J. 21, 4101-4111
- 17. Treiber, K., Singer, A., Henke, B., and Müller, W. E. (2005) Br. J. Pharmacol. 145, 75-83
- 18. Rheinwald, J. G., and Green, H. (1975) Cell 6, 317-330
- 19. Schempp, C. M., Kiss, J., Kirkin, V., Averbeck, M., Simon-Haarhaus, B., Kremer, B., Termeer, C. C., Sleeman, J., and Simon, J. C. (2005) Planta Med. 71, 999-1004
- 20. Bikle, D. D., Ratnam, A., Mauro, T., Harris, J., and Pillai, S. (1996) J. Clin. Investig. 97, 1085-1093
- 21. Gerdes, J., Lemke, H., Baisch, H., Wacker, H. H., Schwab, U., and Stein, H. (1984) J. Immunol. 133, 1710-1715
- 22. Hofmann, T., Schaefer, M., Schultz, G., and Gudermann, T. (2002) Proc. Natl. Acad. Sci. U. S. A. 99, 7461-7466
- 23. Sharpe, G. R., Gillespie, J. I., and Greenwell, J. R. (1989) FEBS Lett. 254, 25 - 28
- 24. Beck, B., Lehen'kyi, V., Roudbaraki, M., Flourakis, M., Charveron, M., Bordat, P., Polakowska, R., Prevarskaya, N., and Skryma, R. (2008) Cell Calcium 43, 492-505
- 25. Lehen'kyi, V., Beck, B., Polakowska, R., Charveron, M., Bordat, P., Skryma, R., and Prevarskaya, N. (2007) J. Biol. Chem. 282, 22582-22591
- 26. Li, Y., Jia, Y. C., Cui, K., Li, N., Zheng, Z. Y., Wang, Y. Z., and Yuan, X. B. (2005) Nature 434, 894 – 898
- 27. Winn, M. P., Conlon, P. J., Lynn, K. L., Farrington, M. K., Creazzo, T., Hawkins, A. F., Daskalakis, N., Kwan, S. Y., Ebersviller, S., Burchette, J. L., Pericak-Vance, M. A., Howell, D. N., Vance, J. M., and Rosenberg, P. B. (2005) Science 308, 1801-1804
- 28. Forslind, B. (1987) *Acta Dermato-Venereol.* **134,** (suppl.) 1–8
- Menon, G. K., Grayson, S., and Elias, P. M. (1985) J. Investig. Dermatol. 84,
- 30. Elias, P. M., Nau, P., Hanley, K., Cullander, C., Crumrine, D., Bench, G., Sideras-Haddad, E., Mauro, T., Williams, M. L., and Feingold, K. R. (1998) J. Investig. Dermatol. 110, 399-404
- 31. Menon, G. K., and Elias, P. M. (1991) Arch. Dermatol. 127, 57-63
- 32. Pallon, J., Malmqvist, K. G., Werner-Linde, Y., and Forslind, B. (1996) Cell. Mol. Biol. (Noisy-Le-Grand) 42, 111-118
- 33. M., Ahn, S. K., Menon, G. K., Choi, E. H., and Lee, S. H. (2001) Int.J.



- Dermatol. 40, 223-231
- 34. Müller, W. E. (2003) Pharmacol. Res. 47, 101-109
- 35. Maisenbacher, P., and Kovar, K. A. (1992) Planta Medica 58, 351–354
- 36. Schempp, C. A., Windeck, T., Hezel, S., and Simon, J. C. (2003) *Phytomedicine* 10, 31–37
- 37. Gurevich, A. I., Dobrynin, V. N., Kolosov, M. N., Popravko, S. A., Ryabova,
- I. D., Chernov, B. K., Derbents, N. A., Aizenman, B. E., and Garaguly, A. D. (1971) *Antibiotiki* 16, 510 –513
- 38. Schempp, C. M., Winghofer, B., Ludtke, R., Simon-Haarhaus, B., Schopf, E., and Simon, J. C. (2000) *Br. J. Dermatol.* **142,** 979 –984
- 39. Schempp, C. M., Pelz, K., Wittmer, A., Schopf, E., and Simon, J. C. (1999) *Lancet* **353**, 2129

